Effective Locking ~~for Various Phosphorus Pollutants in Water Bodies: of~~ Organophosphate by Lanthanum/Aluminum-Hydroxide Composite

Rui Xu[†, ‡], Meiyi Zhang[*, †], and Gang Pan[*, †, ‡, §]

[†] Research Center for Eco-Environmental Sciences, Chinese Academy of Sciences, Beijing 100085, China

[‡] University of Chinese Academy of Sciences, Beijing 100049, China

[§] School of Animal, Rural and Environmental Sciences, Nottingham Trent University, Brackenhurst Campus, Nottinghamshire NG25 0QF, United Kingdom

* Corresponding author: myzhang@rcees.ac.cn, gpan@rcees.ac.cn

Commented [PG1]:

ABSTRCT: Lanthanum-bearing materials have been widely used to remove phosphorus (P) especially orthophosphate in water treatment. However, its binding ability and interaction mechanism to other P species in natural waters such as organic phosphate and condensed phosphate are not well understood. Here, a lanthanum/aluminum-hydroxide (LAH) composite was used to investigate its adsorption efficiencies and mechanisms to myo-inositol hexakisphosphate (IHP) and pyrophosphate (Pyro-P) with the contrast of orthophosphate (Ortho-P). The maximum IHP and Pyro-P adsorption capacities by LAH were 36.4 mg P g^{-1} and 21.8 mg P g^{-1}, respectively. Zeta potential, ^{31}P solid-state nuclear magnetic resonance (NMR) spectroscopy and P K-edge X-ray absorption near edge structure (XANES) analyses possibly indicated that the interaction between LAH and P species was surface adsorption by the formation of inner-sphere complexes. Liner combination fitting results of XANES showed that IHP and Pyro-P were preferentially bonded with La-hydroxide in LAH under alkaline conditions (pH 8.5). This work elucidates the adsorption properties and mechanisms of IHP and Pyro-P on lanthanum bearing compounds at the molecular level, indicating that LAH was a promising material for eutrophication control.

Keywords: phosphorus, adsorption, XANES, mechanism, eutrophication control

TOC

Formatted: Highlight

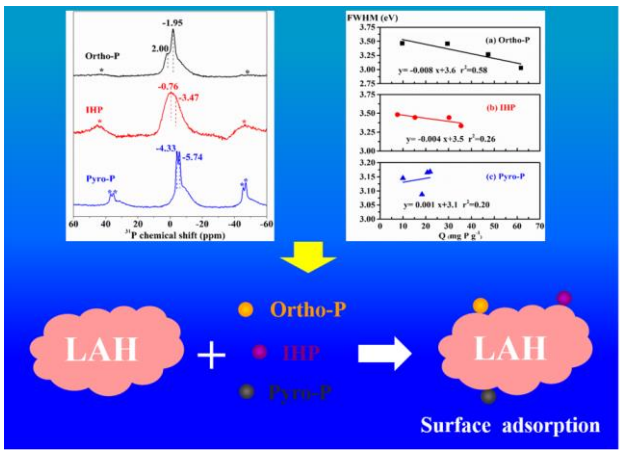

1. INTRODUCTION

Phosphorus (P) is an essential nutrient for biological organisms, but excessive P input is a main factor to trigger eutrophication in freshwater and coastal ecosystem.[1, 2] Over recent decades, great efforts have been made in developing ecologically benign and cost-effective P removal materials.[3] In particular, lanthanum (La) bearing materials have been considered as a useful tool to control P enrichment in lake restoration, owing to its superior P adsorption capacity, low P release rate, and wide applied pH range.[4-7] Previous studies of P removal using La-bearing materials primarily focused on locking inorganic phosphate i.e. orthophosphate (Ortho-P), which is one of the most predominant P species in aquatic ecosystem and can be used by bacteria, algae, and aquatic plants directly.[8-10]

In addition to bioavailable Ortho-P, there are several other species of dissolved P existed in water bodies, such as organic phosphate and condensed phosphate (pyro-, meta-, and polyphosphate).[11] Myo-inositol hexakisphosphate (IHP) is the most abuntant organic phosphate in lake sediments.[12, 13] It can be released into waters under anaerobic conditions and can be used by aquatic organims indirectly.[14] Condensed phosphate for example sodium pyrophosphate (Pyro-P) is widely applied as fertilizers

in soils and may enter waters through leaching and surface runoff.[15] Furthemore, organic phosphate and condensed phosphate can be hydrolyzed to Ortho-P by extracellular phosphatase or phytases and then may be used as potentially bioavailable P pool for aquatic organisms.[11, 16, 17] Such accumulation of various P species may finally increase the environmental risk of eutrophication.[18] Hence, it is necessary to focus on different P species except for Ortho-P to mitigate eutrophication in geo-engineering for lake restoration.

The binding properties of P species on the adsorption materials possibly dominate their behaviors in water bodies. It has been reported that organic phosphate and condensed phosphate are adsorbed on Fe- (hydro)oxide, Al- (hydro)oxide, and titanium dioxide by forming inner-sphere complexes.[19-21] However, little information is available about the fate of organic phosphate and condensed phosphate after La-bearing materials application in aquatic environments. Such lacking of P binding properties with lake restoration materials is not beneficial to understand the potential influence of La-bearing materials and P migration process in water bodies.

Solid state nuclear magnetic resonance (SSNMR) spectroscopy is a versatile technique to study the binding mode of different P species on environmental materials, for instance P bonded on iron oxyhydroxides,[22] gibbsite and kaolinite,[23] and amorphous aluminum hydroxide.[24] X-ray absorption near edge structure (XANES) spectroscopy can provide detail information on local chemical environment of the specific element, which has been widely used to distinguish various P species in soils and sediments.[25, 26] By using the element-specific and in situ techniques of ^{31}P SSNMR and P K-edge XANES, we can obtain the molecular level information of different P species associated with La-bearing materials and predict their performance when application in aquatic environments

Our recent study has demonstrated that lanthanum/aluminum hydroxide composite (LAH) exhibited highly effective adsorption capacity of Ortho-P.[10] These observations promote the hypothesis that LAH may also show an affinity to IHP and Pyro-P existed in water bodies. The objective of this study is to investigate the removal properties of LAH to IHP and Pyro-P and illustrate their adsorption mechanisms at the molecular level. The properties of three P compounds associated with LAH, including potassium dihydrogen phosphate, inositol hexakisphosphate acid sodium salt, and sodium pyrophosphate, were studied by batch experiments and multiple characterization techniques. The experiments of adsorption isotherm, desorption behavior, and adsorption kinetics were conducted to determine the macroscopic binding properties of three P species on LAH. ^{31}P SSNMR and P K-edge XANES techniques were used to explore the microstructures of P bonded on LAH. Liner combination fitting (LCF) analysis was used to investigate the P distribution proportions with La-hydroxide and Al-hydroxide in LAH. The results of our study has demonstrated the interaction mechanism of IHP and Pyro-P with LAH, which is important to design and implement La-bearing materials for eutrophication control.

2. MATERIALS AND METHODS

2.1. Materials.

Three species of P were used in this study, including potassium dihydrogen phosphate (KH_2PO_4, Ortho-P), inositol hexakisphosphate acid sodium salt ($C_6H_9Na_9O_{24}P_6$, IHP), and sodium pyrophosphate ($Na_4P_2O_7 \cdot 10H_2O$, Pyro-P). All reagents were obtained from sigma-aldrich (Saint Louis, MO, USA). The commercial product Phoslock was purchased from Phoslock Water Solutions Ltd., Australia.

2.2. Preparation of LAH.

LAH was synthesized using the same method described in our previous study.[10]

Amounts of analytical grade $LaCl_3 \cdot 7H_2O$ and $AlCl_3$ were dissolved in 200 mL deionized water to obtain a La/Al molar ratio of 1:10 and followed by adding 2 mol L^{-1} NaOH solution at 60 °C until pH 9.0. Then the mixture was stirred at 60 °C for another 2 h. Precipitates were aged for 24 h, then separated by centrifugation, washed with deionized water, and freeze-dried for 24 h. The La mass proportion of LAH was 13.1%.[10] Powders of $La(OH)_3$ and $Al(OH)_3$ were synthesized by the same process to act as controls.[10] The detailed characterizations of LAH were published in our previous studies.[10]

2.3. Adsorption and desorption experiments.

The P adsorption experiments were conducted in 50 mL polypropylene tubes at 25 °C. LAH (1 g L^{-1}) was mixed with various concentrations of P solutions in 0.01 mol L^{-1} NaCl background. The solution pH was adjusted to 8.5 ± 0.05 with 0.10 mol L^{-1} HCl and 0.10 mol L^{-1} NaOH and shaken at 170 rpm at 25 °C for 48 h. Zeta (ζ) potentials of LAH samples after P adsorption were measured by a Zetasizer Nano ZS potential analyzer (Malvern, United Kingdom). The P adsorption capacities of LAH and Phoslock were also determined with initial P concentration 1 mmol L^{-1} at pH 8.5 ± 0.05 under 0.01 mol L^{-1} NaCl background.

In order to explore P desorption capacity of LAH, the desorption experiments were conducted. Adsorbents (1 g L^{-1}) were added to 50 mL polypropylene tubes with initial P concentration 1 mmol L^{-1} in 0.01 mol L^{-1} NaCl background. The solution pH was adjusted to 8.5 ± 0.05 and shaken at 25 °C for 48 h. After the adsorption equilibrium was reached, the exhausted solutions were centrifuged to preserve 10 mL suspension at the bottom, and 0.01 mol L^{-1} NaCl solution was added to keep the same ionic strength. The experimental conditions of desorption experiments were carried out the same as former adsorption studies.

The concentrations of Ortho-P were measured by ascorbic acid method using a UV-756 PC spectrophotometer at 880 nm (Shanghai Sunny Hengping Scientific Instrument CO. Ltd., China). IHP and Pyro-P were hydrolyzed to inorganic phosphate by persulfate acid digestion and then determined using the same method as Ortho-P.[27, 28]

2.4. Adsorption kinetic experiments.

The adsorption kinetic experiments were carried out with initial P concentration 1 mmol L^{-1} in 0.01 mol L^{-1} NaCl background. The solution pH was maintained at 8.5 ± 0.05 and the contact time was from 0 h to 48 h. The samples were taken over a period of time and filtered through a 0.45 μm syringe nylon-membrane filter. The P concentration was determined as the former method in adsorption and desorption experiments.

2.5. Solid-state ^{31}P nuclear magnetic resonance measurements.

Solid-state ^{31}P nuclear magnetic resonance (NMR) spectra of LAH adsorption samples were obtained on a 600 MHz JNM-ECZ600R/M1 spectrometer (14.1 T) at ambient temperature (22 °C). The ^{31}P operating frequency was 242.95 MHz. Samples were contained in 3.2 mm (o.d.) ZrO_2 rotors at a spinning rate of 10 kHz. The ^{31}P spectra were obtained with an excitation 40° pulse of 0.1 μs with a 2 s relaxation delay. The pulse delay was optimized at 2 s to obtain an optimal signal-to-noise ratio.

2.6. P K-edge XANES data collection and analysis.

All XANES spectra were obtained in fluorescence yield mode at Beamline 4B7A at the Beijing Synchrotron Radiation Facility (BSRF), China. Measurements were conducted at energy ranging from −30 to +90 eV relative to P K-edge energy at 2152 eV with a minimum step size of 0.2 eV between 2140 and 2180 eV. Each spectrum was baseline corrected and normalized by ATHENA program.[29] The proportions of

Ortho-P, IHP, and Pyro-P bonded on La- and Al- hydroxides in LAH samples were determined by liner combination fitting (LCF) analysis. Samples of three P compounds bonded on contrast adsorbents $La(OH)_3$ and $Al(OH)_3$ with Ortho-P (30.9 mg P g^{-1} La/15.7 mg P g^{-1} Al), IHP (30.8 mg P g^{-1} La/18.7 mg P g^{-1} Al) and Pyro-P (13.0 mg P g^{-1} La/14.7 mg P g^{-1} Al) were used as standards in LCF analysis, respectively.

3. RESULTS

3.1. Phosphate adsorption and desorption.

The IHP and Pyro-P adsorption isotherms for LAH were L-curves (Figure 1) and were fitted to Langmuir equation with r^2 values of 0.999 and 0.999, respectively (Table S1). The maximum IHP and Pyro-P adsorption capacities by LAH were 36.4 mg P g^{-1} and 21.8 mg P g^{-1}, respectively. The ratio of Q_m (Ortho-P)/Q_m (IHP) was 1.9, suggesting that IHP may bind on LAH surface through two of its six phosphate groups and with the other four phosphate groups free and dissociated. Compared to commercial product Phoslock, the Ortho-P, IHP, and Pyro-P adsorption capacities of LAH were 2.7, 1.1, and 3.0 times higher than those of Phoslock at initial P concentration 1 mmol L^{-1} at pH 8.5, respectively (Figure S1).

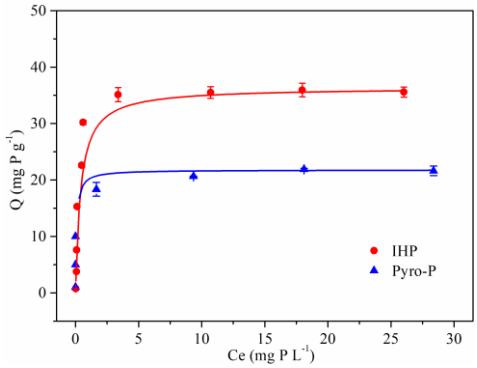

Figure 1. Langmuir adsorption isotherms of IHP and Pyro-P on LAH. The

experimental condition: temperature =25°C, adsorbent dosage =1 g L^{-1}, pH =8.5, and reaction time =48 h.

The ζ potentials of LAH samples after P adsorption all showed a decreasing trend with increasing P adsorption amounts (Figure 2). Additionally, LAH samples with IHP bonded had relatively lower ζ potentials than those of Ortho-P (Figure 2). The P desorption on LAH was also conducted at initial P concentration 1 mmol L^{-1} at pH 8.5 (Figure S2). The results showed that the desorption rates of Ortho-P, IHP, and Pyro-P of LAH were 0.16%, 0.28%, and 0.40% (Figure S2), respectively.

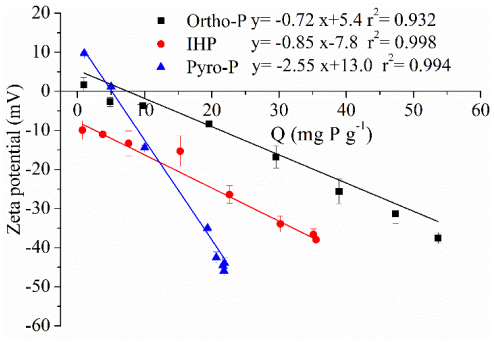

Figure 2. The ζ potentials of LAH after Ortho-P, IHP, and Pyro-P adsorption as a function of total P bonded amounts. Regression fits to the data are shown as solid lines.

3.2. Phosphate adsorption kinetics.

The adsorption kinetic studies of LAH with Ortho-P, IHP, and Pyro-P were shown in Figure 3. The P adsorption capacities of LAH all increased with contacting time and then kept equilibrium. Ortho-P, IHP, and Pyro-P bonded on LAH reached equilibrium after 24 h, 20 h, and 24 h at initial P concentration 1 mmol L^{-1} (Figure 3a), respectively. The adsorption of Ortho-P, IHP, and Pyro-P followed the pseudo-second order kinetics with r^2 values of 0.999, 0.999, and 0.997 (Table S2), respectively. The rate constants (K) of LAH with Ortho-P, IHP, and Pyro-P were 0.052, 0.064, and

187 0.052 g mg^{-1} h^{-1}, respectively.

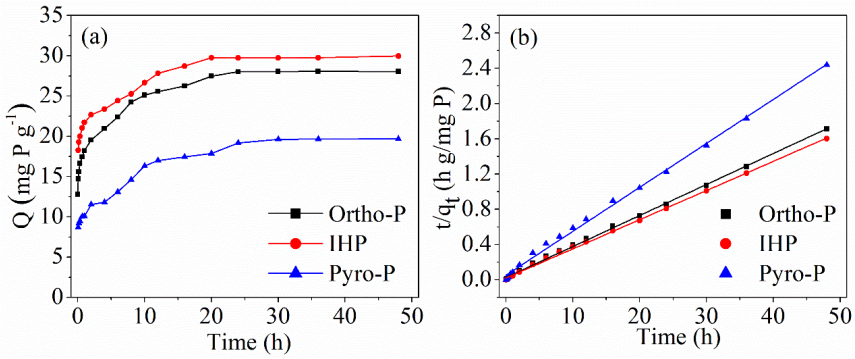

188

189 **Figure 3.** Kinetic studies for Ortho-P, IHP, and Pyro-P adsorption on LAH (a) and its
190 pseudo-second-order fitting plots (b). The experimental condition: temperature =25°C,
191 adsorbent dosage =1 g L^{-1}, pH =8.5, and reaction time =48 h.

192 **3.3. Solid-state ^{31}P NMR.**

193 The ^{31}P SSNMR spectra for P bonded on LAH were shown in Figure 4. The ^{31}P
194 NMR spectrum of Ortho-P bonded on LAH had two major resonances with chemical
195 shifts at δ_{P-31} = 2.00 and -1.95 ppm. The ^{31}P NMR spectrum of IHP bonded on LAH
196 exhibited a main peak at δ_{P-31} = -0.76 ppm with a shoulder at δ_{P-31} = -3.47 ppm. The
197 spectrum for Pyro-P bonded on LAH showed two major peaks at δ_{P-31} = -4.33 and
198 -5.74 ppm.

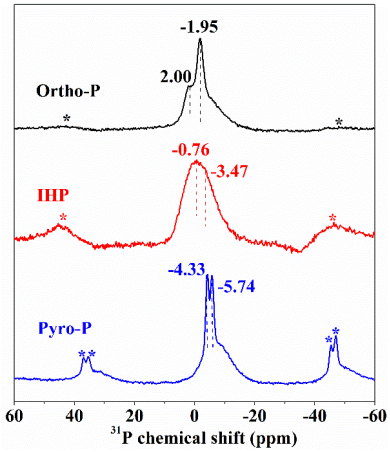

Figure 4. Solid-state ^{31}P NMR spectra of Ortho-P, IHP, and Pyro-P bonded on LAH with initial P concentration 2 mmol L^{-1} at pH 8.5.

3.4. P K-edge XANES.

Normalized P K-edge XANES spectra for Ortho-P, IHP, and Pyro-P bonded on LAH were shown in Figure S3. The full width at half-maximum height (fwhm) of white-line peaks of XANES spectra for P bonded on LAH as a function of P adsorbed amounts were shown in Figure 5. The trends indicated that there were no positive correlations between the fwhm and Ortho-P, IHP, and Pyro-P due to the low r^2 values (0.58, 0.26, and 0.20, respectively) for linear regressions.

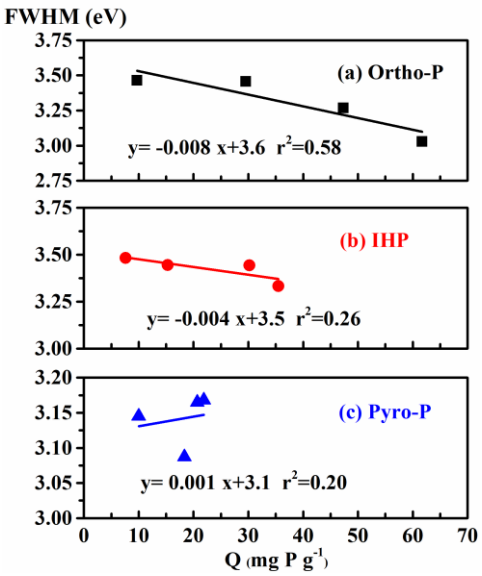

209

210 **Figure 5.** The fwhm of the white-line peaks of XANES spectra for Ortho-P (a), IHP

211 (b), and Pyro-P (c) bonded on LAH as a function of P adsorbed amounts. Regression

212 fits to the data are shown as solid lines.

Commented [PG2]: Only 4 points, may be a problem. Consider move to SI?

213 According to our previous study, LAH were mainly composed of $Al(OH)_3$ and

214 $La(OH)_3$.[10] The distribution proportions of Ortho-P, IHP, and Pyro-P bonded on

215 La-hydroxide and Al-hydroxide were determined using LCF analysis.[30, 31] LCF results

216 showed that the proportions of Ortho-P bonded with La-hydroxide (La-P) were 51.4%

217 - 91.2%, which were higher than those with Al-hydroxide (Al-P) of 48.6% - 8.8%

218 (Figure 6 a1-a4). For LAH samples with IHP bonded, the proportions of IHP

219 associated with La-hydroxide (La-P, 74.5% - 94.5%) were much higher than those

220 with Al-hydroxide (Al-P, 25.5% - 5.5%) (Figure 6 b1-b4). Additionally, the

221 proportions of Pyro-P bonded with La-hydroxide (La-P, 59.1% - 89.3%) in LAH were

222 also higher than those with Al-hydroxide (Al-P, 40.9% - 10.7%) (Figure 6 c1-c4).

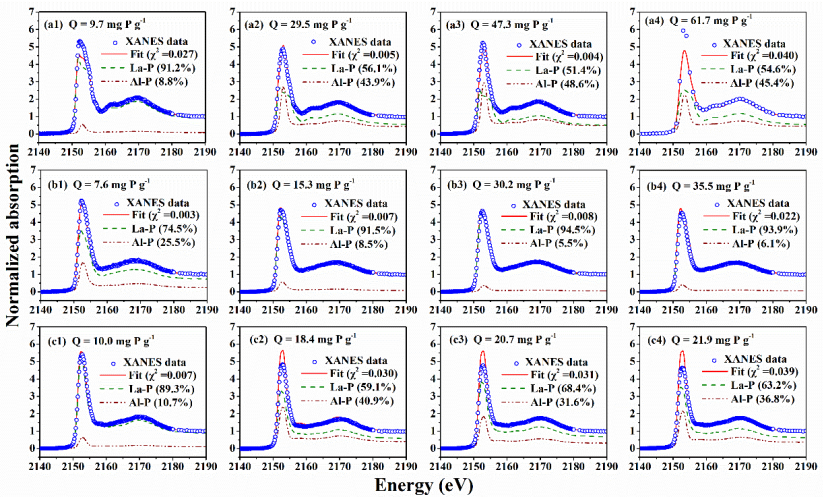

Figure 6. Linear combination fitting for LAH samples after Ortho-P (a), IHP (b), and Pyro-P (c) adsorption with weighted components of La-P and Al-P.

4. DISCUSSION

4.1. Phosphate adsorption on LAH

Compared to the positive ζ potential of pristine LAH (+10 mV) at pH 8.5,[10] the ζ potentials of LAH samples with Ortho-P, IHP, and Pyro-P bonded all decreased with increasing P adsorbed amounts (Figure 2). The results might suggest that three P species were bonded on LAH surfaces by forming inner sphere complexes.[32, 33] The ζ potentials of LAH samples with Ortho-P, IHP, and Pyro-P bonded were linearly related to the total P adsorbed amounts with r^2 values of 0.932, 0.998, and 0.994 (Figure 2), respectively. Such trends of ζ potentials indicated that the process of surface adsorption occurred in the reaction between LAH and three P species.[34] Because if surface precipitation dominated in the interaction process, there would be no significant change in the surface groups responsible for surface charge i.e. ζ potentials.[34] Additionally, the adsorption kinetics of Ortho-P, IHP, and Pyro-P were all fitted to the pseudo-second-order model (Table S2), possibly suggesting that the

process of P adsorption on LAH might be chemisorption.[35] For the ^{31}P SSNMR spectra, it was reported that the chemical shifts of nonreacted Ortho-P, IHP, and Pyro-P appeared at δ_{P-31} = 1.31, -0.5, and -4.65 ppm, respectively.[24, 36] In this study, the peaks in the ^{31}P SSNMR spectra of Ortho-P, IHP, and Pyro-P bonded on LAH at δ_{P-31} = 2.00, -0.76, and -4.33 ppm could thus be assigned to the free phosphate groups adsorbed on LAH. While the peaks at δ_{P-31} = -1.95, -3.47, and -5.74 ppm could be attributed to the phosphate groups bonded on LAH (Figure 4), respectively.[19, 37, 38] Some studies have demonstrated that surface precipitates was shifted to high negative field (δ_{P-31} = -11 to -30 ppm) and signals appearing between 0 and -11 ppm were due to inner-sphere complexes.[37] Hence, the results of ^{31}P NMR analysis further indicated that the formation of inner-sphere P surface complexes was the dominant mechanism on LAH surfaces.

In order to illustrate the mechanism of surface adsorption at the molecular level, we have determined the P K-edge XANES spectra (Figure S3) and calculated the fwhm of white-line peaks of XANES spectra for samples of Ortho-P, IHP, and Pyro-P bonded on LAH (Figure 5). The fwhm values of spectra for Ortho-P, IHP, and Pyro-P bonded on LAH showed no positive correlations with the total P sorbed amounts (Figure 5), respectively. It was reported that surface precipitate of Al-phosphate was formed on the basis of the evidence that the fwhm of the white-line peaks in XANES spectra for Ortho-P bonded on boehmite, non-xl Al-hydroxide or goethite-boehmite mixtures positively correlated with increasing total Ortho-P sorbed amounts.[31] The XANES information possibly provided strong evidence that it is surface adsorption not precipitation played a role in the adsorption of Ortho-P, IHP, and Pyro-P by LAH. In our previous study, we have found that there were oxygen defects on LAH surfaces, which might provide special adsorption sites to Ortho-P.[10] Hence, we could infer that

these oxygen defects might also present as active adsorption sites for IHP and Pyro-P.

Adsorption isotherm results showed that IHP could bond on LAH surfaces through two of its six phosphate groups (Table S1), thus resulting in more negative surface charge of LAH with adsorbed IHP than those of Ortho-P (Figure 2). Owing to the much stronger negative surface charge of IHP,[39] it could be removed a little faster (20 h, Figure 3) via stronger electrostatic attraction compared to Ortho-P and Pyro-P (24 h, Figure 3). However, because IHP had a larger molecule size and stronger steric hindrance than Ortho-P,[40, 41] the maximum IHP binding capacity of LAH (36.4 mg P g^{-1}, Table S1) was less than that of Ortho-P (70.4 mg P g^{-1}).[8] Moreover, LAH had the lowest adsorption capacity of Pyro-P (21.8 mg P g^{-1}, Table S1), which possibly because that Pyro-P had a weaker metal-complexing power owing to its cyclic structure.[42]

4.2. P distribution on LAH

The distribution proportions of Ortho-P, IHP, and Pyro-P bonded on La-hydroxide and Al-hydroxide in LAH were obtained by LCF analysis.[25, 43] The proportion of Ortho-P associated with La-hydroxide were 10.4 times higher than that with Al-hydroxide when total Ortho-P adsorbed amount was 9.7 mg P g^{-1} at pH 8.5 (Figure 6a1). With increasing Ortho-P adsorbed amounts (29.5, 47.3, and 61.7 mg P g^{-1}, respectively), the proportions of Ortho-P bonded with La-hydroxide were 1.3, 1.1, and 1.2 times higher than those with Al-hydroxide (Figure 6a2-a4). The fitting data about Ortho-P indicated that the adsorption active sites on La-hydroxide might tend to become saturated compared to lower Ortho-P adsorbed amount (9.7 mg P g^{-1}). For IHP, it was reported that IHP was initially adsorbed on amorphous Al-hydroxide and then transformed to surface precipitates from pH 3.5 to pH 7.0.[24] In this study, according to P K-edge XANES and ^{31}P SSNMR analyses, our work demonstrated that

IHP always showed a more preferable distributions on La-hydroxide (74.5% - 94.5%, Figure 6b) than those with Al-hydroxide (25.5% - 5.5%, Figure 6b) in LAH via surface adsorption at alkaline condition pH 8.5. Additionally, Pyro-P was preferentially bonded with La-hydroxide at pH 8.5 depending on the higher Pyro-P proportions associated with La-hydroxide (59.1% - 89.3%, Figure 6c) than those of Al-hydroxide (40.9% - 10.7%, Figure 6c). The LCF analysis showed that La-hydroxide had a remarkable P binding ability to different P species at the molecular level. The preferences of Ortho-P, IHP, and Pyro-P on La-hydroxide and Al-hydroxide might provide a theoretical guidance to synthesize novel P locking materials for various P species removal in water treatment.

4.3. Environmental implications

The interfacial reactions between different P species (e.g. inorganic phosphate, organic phosphate, and condensed phosphate) and lake restoration materials can greatly influence the transformation, mobility, and dynamics of P and the chemistry of materials in natural systems, thus affecting the biomass production of ecosystems.[44] Our study is the first to determine the adsorption properties and interaction mechanisms of different P species such as Ortho-P, IHP, and Pyro-P on La/Al-hydroxide composite. It advances the knowledge of using La-bearing materials for effective adsorption of different P species. Our previous studies have demonstrated that LAH had the highest Ortho-P adsorption capacity at pH 4.0 and relatively lower Ortho-P adsorption capacity at pH 8.5.[10] In this study, all the experiments were conducted at pH 8.5. The results showed that LAH also has excellent adsorption capacities to IHP and Pyro-P compared to commercial available Phoslock (Figure S1), which could significantly control the concentration of total P in water bodies and block excessive P source for aquatic organisms growing. Owing to higher P binding

ability to La-hydroxide (Figure 6), LAH exhibited low P desorption rates at typical lake pH 8.5 (Figure S2). Our work has demonstrated that P was bonded on LAH surface via adsorption mechanism not surface precipitation, which might be a stable P storage from the view of P recycling. To better understand the environmental behavior of LAH when using in geo-engineering lake restoration, further studies with respect to the interaction between LAH and different P species dissolved from sediments should be taken into account.[45] According to LCF analysis, we can exactly determine the contribution of La-hydroxide versus Al-hydroxide to different P species in LAH. Such molecular level information could also provide a guide to develop new multifunctional P removal materials in the future.

5. Conclusions

In this study, the removal efficiencies and adsorption mechanisms of IHP and Pyro-P with the contrast of Ortho-P by LAH composite were investigated. The maximum IHP and Pyro-P adsorption capacities by LAH were 36.4 mg P g^{-1} and 21.8 mg P g^{-1}, respectively. The ζ potentials of LAH samples with Ortho-P, IHP, and Pyro-P bonded all decreased with increasing P adsorbed amounts. For the ^{31}P SSNMR spectra, the peaks at δ_{P-31} = -1.95, -3.47, and -5.74 ppm could be attributed to the phosphate groups bonded on LAH, respectively. The trends of fwhm indicated that there were no positive correlations between the fwhm and Ortho-P, IHP, and Pyro-P due to the low r^2 values (0.58, 0.26, and 0.20, respectively) for linear regressions. The LCF analysis showed that La-hydroxide had a remarkable P binding ability to different P species at the molecular level. Zeta potential, NMR spectroscopy and P K-edge XANES analyses possibly indicated that the interaction between LAH and P species was surface adsorption by the formation of inner-sphere complexes.

ASSOCIATED CONTENT

Supporting Information

More detailed information about (1) Langmuir isotherm parameters of LAH (Table S1); (2) pseudo-second-order model constants and correlation coefficients of LAH (Table S2); (3) P adsorption capacities of LAH and Phoslock (Figure S1); (4) P desorption rates to LAH (Figure S2); and (5) normalized XANES spectra of LAH with bonded Ortho-P, IHP, and Pyro-P (Figure S3).

AUTHOR INFORMATION

Corresponding Authors

*E-mail: myzhang@rcees.ac.cn.

*E-mail: gpan@rcees.ac.cn. Tel.: +86 10 62849686; Fax: +86 10 62849686.

Formatted: Italian (Italy)

Field Code Changed

Formatted: Italian (Italy)

Formatted: Italian (Italy)

Notes

The authors declare no competing financial interest.

ACKNOWLEDGEMENTS

This work was supported by the National Key R&D Program of China (2017YFA0207204, 2018YFD0800305), and National Natural Science Foundation of China (21377003). XANES experiments were carried out at beamline 4B7A, Beijing Synchrotron Radiation Facility (BSRF), China. We gratefully appreciate Zheng Lei, Ma Chenyan, and Hu Yongfeng for their assistances with XANES analysis.

REFERENCES

1. Conley, D. J.; Paerl, H. W.; Howarth, R. W.; Boesch, D. F.; Seitzinger, S. P.; Havens, K. E.; Lancelot, C.; Likens, G. E., Controlling eutrophication: nitrogen and phosphorus. *Science* **2009,** *323*, (20), 1014-1015.

2. Smith, V. H.; Tilman, G. D.; Nekola, J. C., Eutrophication: impacts of excess nutrient inputs on freshwater, marine, and terrestrial ecosystems. *Environ. Pollut.*

364 **1999,** *100*, 179-196.

365 3. Douglas, G. B.; Hamilton, D. P.; Robb, M. S.; Pan, G.; Spears, B. M.; Lürling, M.,
366 Guiding principles for the development and application of solid-phase phosphorus
367 adsorbents for freshwater ecosystems. *Aquat. Ecol.* **2016**, 1-21.

368 4. Shin, E. W.; Karthikeyan, K. G.; Tshabalala, M. A., Orthophosphate sorption onto
369 lanthanum treated lignocellulosic sorbents. *Environ. Sci. Technol.* **2005,** *39*, (16),
370 6273-6279.

371 5. Yang, J.; Yuan, P.; Chen, H.-Y.; Zou, J.; Yuan, Z. G.; Yu, C. Z., Rationally
372 designed functional macroporous materials as new adsorbents for efficient phosphorus
373 removal. *J. Mater. Chem.* **2012,** *22*, (19), 9983-9990.

374 6. Yu, J.; Xiang, C.; Zhang, G.; Wang, H.; Ji, Q.; Qu, J., Activation of lattice oxygen
375 in LaFe (Oxy)hydroxides for efficient phosphorus removal. *Environ. Sci. Technol.*
376 **2019,** *53*, (15), 9073-9080.

377 7. Fang, L.; Liu, R.; Li, J.; Xu, C.; Huang, L. Z.; Wang, D., Magnetite/Lanthanum
378 hydroxide for phosphate sequestration and recovery from lake and the attenuation
379 effects of sediment particles. *Water Res.* **2018,** *130*, 243-254.

380 8. Smith, V. H., *Cultural eutrophication of inland, estuarine, and coastal waters*.
381 Springer: New York, 1998; p 7-49.

382 9. Ahlgren, J.; Reitzel, K.; Danielsson, R.; Gogoll, A.; Rydin, E., Biogenic
383 phosphorus in oligotrophic mountain lake sediments: differences in composition
384 measured with NMR spectroscopy. *Water Res.* **2006,** *40*, (20), 3705-3712.

385 10. Xu R.; Zhang M. Y.; Robert J.G. Mortimer; Pan, G., Enhanced phosphorus

386 locking by novel lanthanum/aluminum− hydroxide composite: Implications for
387 eutrophication control. *Environ. Sci. Technol.* **2017,** *51*, (6), 3418-3425.
388 11. Correll, D. L., The role of phosphorus in the eutrophication of receiving waters: A
389 review. *J. Environ. Qual* **1998,** *27*, (2), 261-266.
390 12. Groot, C. J. D.; Golterman, H. L., On the presence of organic phosphate in some
391 Camargue sediments: evidence for the importance of phytate. *Hydrobiologia* **1993,**
392 *252*, (1), 117-126.
393 13. Turner, B. L.; Cheesman, A. W.; Godage, H. Y.; Riley, A. M.; Potter, B. V.,
394 Determination of neo- and D-chiro-inositol hexakisphosphate in soils by solution ^{31}P
395 NMR spectroscopy. *Environ. Sci. Technol.* **2012,** *46*, (9), 4994-5002.
396 14. Suzumura M.; A., K., Mineralization of inositol hexaphosphate in aerobic and
397 anaerobic marine sediments: Implications for the phosphorus cycle. *Geochimica et*
398 *Cosmochimica Acta* **1995,** *59*, (5), 1021-1026.
399 15. R.P. Dick; Tabatabai, M. A., Polyphosphates as sources of phosphorus for plants.
400 *Fertilizer Research* **1987,** *12*, (2), 107-118.
401 16. Ignacio Hernandez; Abraham P ´erez-Pastor; ´ens, J. L. P. e. L., Ecological
402 significance of phosphomonoesters and phosphomonoesterase activity in a small
403 Mediterranean river and its estuary. *Aquatic Ecology* **2000,** *34*, (2), 107-117.
404 17. Dyhrman, S. T.; Chappell, P. D.; Haley, S. T.; Moffett, J. W.; Orchard, E. D.;
405 Waterbury, J. B.; Webb, E. A., Phosphonate utilization by the globally important
406 marine diazotroph Trichodesmium. *Nature* **2006,** *439*, (7072), 68-71.
407 18. Sundareshwar;, P. V.; Morris;, J. T.; Pellechia;, P. J.; Cohen;, H. J.; Porter;, D. E.;

Jones, B. C., Occurrence and ecological implications of pyrophosphate in estuaries. *Limnol. Oceanogr.* **2001,** *46*, (6), 1570-1577.

19. Wan, B.; Yan, Y. P.; Liu, F.; Tan, W. F.; He, J. J.; Feng, X. H., Surface speciation of *myo*-inositol hexakisphosphate adsorbed on TiO_2 nanoparticles and its impact on their colloidal stability in aqueous suspension: A comparative study with orthophosphate. *Sci. Total. Environ.* **2016,** *544*, 134-142.

20. Yan, Y.; Koopal, L. K.; Li, W.; Zheng, A.; Yang, J.; Liu, F.; Feng, X., Size-dependent sorption of myo-inositol hexakisphosphate and orthophosphate on nano-gamma-Al2O3. *Journal of colloid and interface science* **2015,** *451*, 85-92.

21. Guan, X. H.; Liu, Q.; Chen, G. H.; Shang, C., Surface complexation of condensed phosphate to aluminum hydroxide: an ATR-FTIR spectroscopic investigation. *Journal of colloid and interface science* **2005,** *289*, (2), 319-27.

22. Kim, J.; Li, W.; Philips, B. L.; Grey, C. P., Phosphate adsorption on the iron oxyhydroxides goethite (α-FeOOH), akaganeite (β-FeOOH), and lepidocrocite (γ-FeOOH): a 31P NMR Study. *Energy & Environmental Science* **2011,** *4*, (10), 4298-4305.

23. Van Emmerik, T. J.; Sandström, D. E.; Antzutkin, O. N.; Angove, M. J.; Johnson, B. B., ^{31}P solid-state nuclear magnetic resonance study of the sorption of phosphate onto gibbsite and kaolinite. *Langmuir* **2007,** *23*, (6), 3205-3213.

24. Yan, Y.; Li, W.; Yang, J.; Zheng, A.; Liu, F.; Feng, X.; Sparks, D. L., Mechanism of myo-inositol hexakisphosphate sorption on amorphous aluminum hydroxide: spectroscopic evidence for rapid surface precipitation. *Environmental science &*

430 *technology* **2014,** *48*, (12), 6735-42.
431 25. Liu, J.; Hu, Y. F.; Yang, J. J.; Abdi, D.; Cade-Menun, B. J., Investigation of soil
432 legacy phosphorus transformation in long-term agricultural fields using sequential
433 fractionation, P K-edge XANES and solution P NMR spectroscopy. *Environ. Sci.*
434 *Technol.* **2015,** *49*, (1), 168-176.
435 26. Werner, F.; Prietzel, J., Standard Protocol and Quality Assessment of Soil
436 Phosphorus Speciation by P K-Edge XANES Spectroscopy. *Environmental science &*
437 *technology* **2015,** *49*, (17), 10521-8.
438 27. Martin, M.; Celi, L.; Barberis, E., Determination of low concentrations of organic
439 phosphorus in soil solution. *Commun. Soil Sci. and Plan.* **1999,** *30*, (13-14),
440 1909-1917.
441 28. Georgantas, D. A.; Grigoropoulou, H. P., Orthophosphate and metaphosphate ion
442 removal from aqueous solution using alum and aluminum hydroxide. *Journal of*
443 *colloid and interface science* **2007,** *315*, (1), 70-9.
444 29. Ravel, B.; Newville, M., ATHENA, ARTEMIS, HEPHAESTUS: data analysis for
445 X-ray absorption spectroscopy using IFEFFIT. *J. Synchrotron Radiat.* **2005,** *12*, (Pt 4),
446 537-541.
447 30. Liu, Y. T.; Hesterberg, D., Phosphate bonding on noncrystalline Al/Fe-hydroxide
448 coprecipitates. *Environ. Sci. Technol.* **2011,** *45*, (15), 6283-6289.
449 31. Khare, N.; Hesterberg, D.; Martin, J. D., XANES investigation of phosphate
450 sorption in single and binary systems of iron and aluminum oxide minerals. *Environ.*
451 *Sci. Technol.* **2005,** *39*, (7), 2152-2160.

452 32. Wan, B.; Yan, Y. P.; Liu, F.; Tan, W. F.; He, J. J.; Feng, X. H., Surface speciation
453 of myo-inositol hexakisphosphate adsorbed on TiO_2 nanoparticles and its impact on
454 their colloidal stability in aqueous suspension: A comparative study with
455 orthophosphate. *Sci. Total Environ.* **2016,** *544*, 134-142.
456 33. Antelo, J.; Avena, M.; Fiol, S.; Lopez, R.; Arce, F., Effects of pH and ionic
457 strength on the adsorption of phosphate and arsenate at the goethite-water interface. *J.*
458 *Colloid Interface Sci.* **2005,** *285*, (2), 476-486.
459 34. Li, L.; Stanforth, R., Distinguishing adsorption and surface precipitation of
460 phosphate on goethite (alpha-FeOOH). *J. Colloid Interface Sci.* **2000,** *230*, (1), 12-21.
461 35. Huang, W. Y.; Li, D.; Liu, Z. Q.; Tao, Q.; Zhu, Y.; Yang, J.; Zhang, Y. M.,
462 Kinetics, isotherm, thermodynamic, and adsorption mechanism studies of
463 $La(OH)_3$-modified exfoliated vermiculites as highly efficient phosphate adsorbents.
464 *Chem. Eng. J.* **2014,** *236*, (2), 191-201.
465 36. Ye Ru han; Chen Yong; Liu Ya Ling; Zhu Li Ming; Li Zheng Quan; Sun Yi Feng;
466 Long, P. W., Analysis of phosphorus-containing compounds in detergents by ^{31}P
467 nuclear magnetic resonance. *Journal of Instrumental Analysis* **2011,** *30*, (6), 624-628.
468 37. Li, W.; Pierre-Louis, A.-M.; Kwon, K. D.; Kubicki, J. D.; Strongin, D. R.; Phillips,
469 B. L., Molecular level investigations of phosphate sorption on corundum (α-Al_2O_3) by
470 ^{31}P solid state NMR, ATR-FTIR and quantum chemical calculation. *Geochim.*
471 *Cosmochim. Ac.* **2013,** *107*, 252-266.
472 38. Sannigrahi, P., Polyphosphates as a source of enhanced P fluxes in marine
473 sediments overlain by anoxic waters: Evidence from ^{31}P NMR. *Geochem. Trans.* **2005,**

474 *6*, (3), 52-59.
475 39. Wan, B.; Yan, Y. P.; Liu, F.; Tan, W. F.; He, J. J.; Feng, X. H., Effects of
476 myo-inositol hexakisphosphate and orthophosphate adsorption on aggregation of
477 CeO_2 nanoparticles: roles of pH and surface coverage. *Environmental Chemistry* **2016,**
478 *13*, (1), 34-42.
479 40. Ruttenberg, K. C.; Sulak, D. J., Sorption and desorption of dissolved organic
480 phosphorus onto iron (oxyhydr)oxides in seawater. *Geochimica et Cosmochimica*
481 *Acta* **2011,** *75*, (15), 4095-4112.
482 41. Yan, Y. P.; Koopal, L. K.; Li, W.; Zheng, A. M.; Yang, J.; Liu, F.; Feng, X. H.,
483 Size-dependent sorption of myo-inositol hexakisphosphate and orthophosphate on
484 nano-gamma-Al_2O_3. *J. Colloid Interface Sci.* **2015,** *451*, 85-92.
485 42. Corbridge, D. E., *Phosphorus: an outline of its chemistry, biochemistry and uses*.
486 Elsevier Science: Netherlands, 1992.
487 43. Andersson, K. O.; Tighe, M. K.; Guppy, C. N.; Milham, P. J.; McLaren, T. I.;
488 Schefe, C. R.; Lombi, E., XANES demonstrates the release of calcium phosphates
489 from alkaline vertisols to moderately acidified solution. *Environ. Sci. Technol.* **2016,**
490 *50*, (8), 4229-4237.
491 44. de Vicente, I.; Jensen, H. S.; Andersen, F. O., Factors affecting phosphate
492 adsorption to aluminum in lake water: implications for lake restoration. *Sci. Total*
493 *Environ.* **2008,** *389*, (1), 29-36.
494 45. Huang, X. L.; Zhang, J. Z., Spatial variation in sediment-water exchange of
495 phosphorus in florida bay: AMP as a model organic compound. *Environ. Sci. Technol.*

2010, *44*, (20), 7790-7795.